Future Network and MobileSummit 2010 Conference Proceedings
Paul Cunningham and Miriam Cunningham (Eds)
IIMC International Information Management Corporation, 2010
ISBN: 978-1-905824-16-8

OFDM and FBMC Performance Comparison for Multistream MIMO Systems

Iñaki ESTELLA[1], Antonio PASCUAL-ISERTE[1,2], Miquel PAYARÓ[1]
[1]*Centre Tecnològic de Telecomunicacions de Catalunya (CTTC), Av. Carl Friedrich Gauss* 7, *Castelldefels, 8860, Barcelona (Spain)*
Tel: +34936452900, *Fax:* +34936452901,
[2]*Department of Signal Theory and Communications, Universitat Politècnica de Catalunya (UPC) , Jordi Girona* 1 − 3, *Barcelona, 08034, Barcelona (Spain)*
Tel: +34934016460, *Fax:* +34934016447,
Email:{inaki.estella, miquel.payaro}@cttc.cat,
antonio.pascual@upc.edu

Abstract: A comparison between two multicarrier (MC) transmission techniques is presented: OFDM, based on cyclic prefix (CP), and FBMC, based on filterbank architecture. Multistream multiple input multiple output (MIMO) techniques that require channel state information (CSI) at the transmitter and receiver, are applied in these schemes to improve their throughput. When perfect CSI is assumed, OFDM presents lower energy-efficiency than FBMC due to the use of the CP. However, unlike OFDM, the use of multiple streams increases interference in FBMC. When imperfect CSI is considered, while there is neither inter-symbol interference (ISI) nor inter-carrier interference (ICI) in OFDM, FBMC still suffers this effect. In scenarios with low coherence bandwidth channels, the performance of FBMC degrades due to a significant increase in interference. On the contrary, OFDM is shown to be more robust in such scenarios. In this paper, we explore analytically and by means of simulation, the sources of errors together with the effects of channel coherence bandwidth and the energy-efficiency trade-off observed for both systems.

Keywords: OFDM, FBMC, MIMO, robust design, channel coherence bandwidth

1. Introduction

Multicarrier (MC) modulations are a key feature in current physical layer system technologies. Broadband systems such as digital subscriber lines (DSL), wireless local area network (WLAN) or future long term evolution (LTE) are designed on the grounds of MC systems, such as OFDM and filter bank multiple carrier (FBMC) [1],[2]. The general feature behind these technologies is the division of the wideband channel into different narrow-band frequency subbands such that each subband can be approximated as a frequency flat channel. Then, the stream to be transmitted is sent divided into lower rate substreams, one per subchannel.

The increasing demand on higher bit rates can be dealt with the inclusion of multiple antennas at transmission and reception, yielding multiple input multiple output (MIMO) systems [3]. In rich scattering environments, MIMO systems enable to create parallel communication channels for each subcarrier, which boosts the capacity performance.

[1]This work was partially supported by the Catalan Government under grants 2009 SGR 1046 and 2009 SGR 891, by the Spanish Government under project TEC2008-06327-C03 (MULTI-ADAPTIVE), and by the European Commission under projects ICT-FP7-211887 (PHYDYAS) and ICT-FP7-216715 (NEWCOM++).

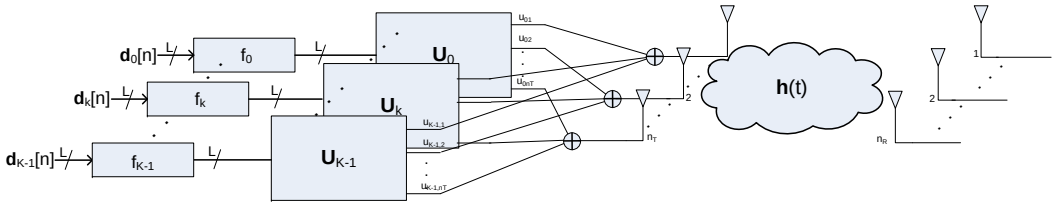

Figure 1: Multistream MC transmitter architecture. The receiver is symmetric. In picture, beamvectors are noted as $\mathbf{U}_k = [\mathbf{u}_{k,1} \dots \mathbf{u}_{k,L}]$ and symbols as $\mathbf{d}_k[n] = [d_{k,1}[n] \dots d_{k,L}[n]]^T$.

It must be highlighted that the design of MIMO schemes depends on the knowledge on the channel state information (CSI). In practical systems, the channel is known through an estimate, that will not be perfect [4]. In [5], the authors analyzed the performance degradation of MIMO-FBMC systems due to channel estimation errors for the single beamforming case. In this paper, we will consider the more complex case of multiple beamforming and we will analyze how the presence of multiple streams per carrier, together with the effects of imperfect CSI and the channel coherence bandwidth, impact on the performance of MIMO-FBMC and MIMO-OFDM schemes.

The rest of the paper is organized as follows. In Section 2, we review the FBMC scheme for multistream MIMO systems. In Section 3, we analyze the error sources in multistream systems with perfect and imperfect CSI. In Section 4, the performance simulations are depicted and conclusions follow in the final section.

2. The multiple beamforming architecture for MIMO-FBMC

Multiple beamforming schemes have proven to be very useful in order to increase throughput in OFDM systems [6]. As pointed out in the introduction, in this paper we extend the multiple beamforming technique for FBMC schemes to improve the performance of such systems.

2.1 Multicarrier MIMO techniques

OFDM is well known in the literature, hence, we focus on the less known modular filterbank schemes (where the FBMC scheme belongs to). From the general set of filterbank schemes, we restrict to uniform filterbanks, i.e., those such that the individual finite-length filters $f_k(t)$ can be expressed as shifted versions of the prototype filter $f_0(t)$[2] :

$$f_k(t) = f_0(t)e^{j2\pi k\Delta f t}, \tag{1}$$

where Δf is the frequency separation between two consecutive filters. This model suits for OFDM assuming a rectangular prototype filter $f_0(t)$ and the inclusion of the CP.

We consider a MC MIMO system with K subcarriers equipped with n_T antennas at the transmitter and n_R antennas at the receiver. The transmitted signal consists of L parallel streams at each carrier k. Each of the streams is filtered by the corresponding filter f_k and subsequently multiplied by the weighting corresponding to the intended antenna, known as beamformer $\mathbf{u}_{k,l} \in \mathbb{C}^{n_T}$ (see Figure 1). Then, all ouputs for the same antenna are added and connected to the corresponding antenna. Thus, the analogical baseband transmitted signal $\mathbf{x}(t)$ can be expressed as:

$$\mathbf{x}(t) = \sum_{n=-\infty}^{\infty} \sum_{k=0}^{K-1} \sum_{l=0}^{L-1} d_{k,l}[n]\mathbf{u}_{k,l} f_k(t - nT), \tag{2}$$

time index - n

Frequency index - k	-4	-3	-2	-1	0	1	2	3	4
-2	0	0.0006	-0.0001	0	0	0	-0.0001	0.0006	0
-1	0.0054	0.0429j	-0.1250	-0.2058j	0.2393	0.2058j	-0.1250	-0.0429j	0.0054
0	0	-0.0668	0.0002	0.5644	1	0.5644	0.0002	-0.0668	0
1	0.0054	-0.0429j	-0.1250	0.2058j	0.2393	-0.2058j	-0.1250	0.0429j	0.0054
2	0	0.0006	-0.0001	0	0	0	-0.0001	0.0006	0

Figure 2: Graphical representation of the time-frequency response of the FBMC filterbank system from the design of Bellanger in [7].

where $d_{k,l}[n]$ denotes the input symbol sequence of the l-th stream in the k-th filter and T is the symbol period. The j-th entry of vector $\mathbf{x}(t)$ represents the signal transmitted through the j-th antenna. Then it is transmitted through the MIMO channel, $\mathbf{h}(t) \in \mathbb{C}^{n_R \times n_T}$, whose (i,j)-th entry contains the channel impulse response from the j-th transmitter to the i-th receiver. The received signal is $\mathbf{y}(t) = \mathbf{h}(t) * \mathbf{x}(t) + \mathbf{w}(t)$, where $*$ denotes the convolution operation and $\mathbf{w}(t) \in \mathbb{C}^{n_R}$ represents the system noise. The received signal is multiplied by the corresponding receiver beamvector $\mathbf{v}_{k,l} \in \mathbb{C}^{n_R}$ and processed through a bank of matched filters, $g_k(t) = f_k^*(-t)$, to obtain the output $r_{k,l}(t) = g_k(t) * (\mathbf{v}_{k,l}^H \mathbf{y}(t))$:

$$r_{k,l}(t) = \sum_{n=-\infty}^{\infty} \sum_{k'=0}^{K-1} \sum_{l'=0}^{L-1} \mathbf{v}_{k,l}^H [g_k(t-nT) * \mathbf{h}(t-nT) * f_{k'}(t-nT)] \mathbf{u}_{k',l'} d_{k',l'}[n] + w'_{k,l}(t), \quad (3)$$

where we have defined the equivalent noise, $w'_{k,l}(t) \equiv \mathbf{v}_{k,l}^H [g_k(t) * \mathbf{w}(t)]$. After analog to digital conversion sampling at $t_n = nT_s + \tau_o$, where τ_o is the delay maximizing the correlation between f_k and g_k. This expression can be approximated at given time n, stream l and frequency k by:

$$r_{k,l}[n] \approx \sum_{n'=-\infty}^{\infty} \sum_{k'=0}^{K-1} \sum_{l'=0}^{L-1} t_{k-k',n-n'} \mathbf{v}_{k,l}^H \mathbf{H}_{k,k'} \mathbf{u}_{k',l'} d_{k',l'}[n'] + w'_{k,l}[n], \quad (4)$$

where $\mathbf{H}_{k,k'}$ is the Fourier transform of the MIMO temporal channel $\mathbf{h}(t)$ at frequency $f = \frac{(k'+k)}{2}\Delta f$ (see Appendix A). The parameter $t_{k,n}$ is known as the transmultiplexer response [2] and it characterizes the ICI and ISI terms centered at k and n when a single symbol $d_{k,l}[n] = 1$ is transmitted through the filterbank system and an ideal channel. The specific values of $t_{k-k',n-n'}$ in this paper are depicted in Figure 2 [7].

From now on, we refer as FBMC for the specific considered scheme, consisting in creating a time-frequency pattern of real and imaginary symbols using an offset *real* PAM modulation and a factor $\theta_{k,n}$ as [8]:

$$d_{k,l}[n] = \theta_{k,n} s_{k,l}[n] = j^{(k+n)} s_{k,l}[n]. \quad (5)$$

To recover the transmitted symbols, the received signal $r_{k,l}[n]$ given in (4) is multiplied by $\theta_{k,n}^*$. and equalized dividing by the estimated equivalent gain $\hat{H}_{k,l} = \mathbf{v}_{k,l}^H \tilde{\mathbf{H}}_{k,k} \mathbf{u}_{k,l}$. In practice, the receiver estimates the channel, and the beamformers $\mathbf{v}_{k,l}$ and $\mathbf{u}_{k,l}$, are designed based on the available estimated channel $\tilde{\mathbf{H}}_{k,k}$. The generated pattern causes the interference at large transmultiplexer values $t_{k,n}$ to be pure imaginary and pure real

at small $t_{k,n}$ values. Then, at detection,

$$\frac{\theta^*_{k,n} r_{k,l}[n]}{\hat{H}_{k,l}} = \frac{H_{k,l}}{\hat{H}_{k,l}} s_{k,l}[n] + \sum_{\substack{l'=0 \\ l' \neq l}}^{L-1} \frac{\mathbf{v}^H_{k,l} \mathbf{H}_{k,k} \mathbf{u}_{k,l'}}{\hat{H}_{k,l}} s_{k,l'}[n] + \\ + \sum_{\substack{(k',n') \in \mathcal{R} \\ (k',n') \neq (0,0)}} \sum_{l'=0}^{L-1} t_{k',n'} \frac{\mathbf{v}^H_{k,l} \mathbf{H}_{k,k-k'} \mathbf{u}_{k-k',l'}}{\hat{H}_{k,l}} (\pm s_{k-k',n-n',l'}) + \\ + j \sum_{\substack{(k',n') \in \mathcal{I} \\ (k',n') \neq (0,0)}} \sum_{l'=0}^{L-1} t_{k',n'} \frac{\mathbf{v}^H_{k,l} \mathbf{H}_{k,k-k'} \mathbf{u}_{k-k',l'}}{\hat{H}_{k,l}} (\pm s_{k-k',n-n',l'}), \quad (6)$$

where $\mathcal{R} = \{(0,2),(0,-2),(2,2),(2,-2),(-2,2),(-2,-2)\}$ and the set $\mathcal{I}$ contains the remaining elements in the set $(k',n') \in [-2,2] \times [-4,4]$, from the table in Figure 2. The $\pm$ notation has been used to indicate the result of $\theta^*_{k,n}\theta_{k-k',n-n'}$. Taking the real part in (6), the ICI and ISI terms in $\mathcal{I}$ can be eliminated whenever $\mathbf{v}^H_{k,l'} \mathbf{H}_{k,k-k'} \mathbf{u}_{k-k',l'} / \hat{H}_{k,l}$ is real, while elements in $\mathcal{R}$ remain negligible.

2.2 Beamforming design

Multistream techniques allow us to send up to a maximum of $L \leq \min\{n_T, n_R\}$ streams per carrier with the possibility to distinguish them at reception. We consider the design of beamformers $\mathbf{u}_{k,l}$ and $\mathbf{v}_{k,l}$ in the high enough coherence bandwidth where ICI and ISI terms are negligible. This is possible for OFDM and an approximation for FBMC systems. Then system (4) can then be modeled by

$$r_{k,l}[n] = \sum_{l'=0}^{L-1} \mathbf{v}^H_{k,l} \mathbf{H}_{k,k} \mathbf{u}_{k,l'} d_{k,l'}[n] + w'_{k,l}[n]. \quad (7)$$

Hence, the design of the L beamformers for carrier k only depends on channel at subband k. A solution for the transmit beamformer design that potentially achieves high throughput for such a channel is derived in [9] and is given by the L right singular vectors associated to the L-th largest singular values $\lambda_{k,l}$ of the Fourier transform MIMO channel matrix, $\mathbf{H}_{k,k}$, $\mathbf{e}^r_{k,l}$, scaled by the square root of the power assigned to stream l in carrier k, $\mathbf{u}_{k,l} = \sqrt{P_{k,l}}\mathbf{e}^r_{k,l}$. The receiver beamformers are the corresponding L orthonormal left singular vectors. Anyway, at receiver any scaling is also correct as it does not modify the SNR. Power can be allocated according to different criteria depending on the performance figure to optimize. We restrict our study to the minimum effective probability of error (MEPE) [9], which has been proved to obtain high performance in FBMC schemes [5].

3. Sources of error in multistream transmissions

When a MC system is used in practice, multiple beamformers lead to inherent additional ISI and ICI terms. Next, we detail the sources for such phenomena.

3.1 Noise

The propagation through the channel introduces noise modeled as zero-mean circular white Gaussian noise with spectral density $N_0/2$ and spatially white at the receiver. After being processed by the receiver bank of filters g_k the power of the effective noise, at the l-th stream in the k-th carrier is, for normalized $\mathbf{v}_{k,l}$, $w_{k,l}(t)$, in (3), can be expressed as $P_{w'_{k,l}} = \int_{-\infty}^{\infty} \frac{N_0}{2}|G_k(f)|^2||\mathbf{v}_{k,l}||^2 df = \int_{-\infty}^{\infty} \frac{N_0}{2}|G_0(f)|^2 df$. Note that it is independent of the beamformer design for orthonormal beamformers and white noise.

3.2 Non-orthogonality in $f_k(t)$ and $g_{k'}(t)$

OFDM systems, use the CP to obtain a Toeplitz channel matrix, that is diagonalized by complex exponential filters $exp(j2\pi kn/K)$, which are orthogonal, i.e. lead to orthogonal subchannels. However, using the CP reduces the efficiency of the modulation.

On the contrary FBMC schemes use non orthogonal $f_k(t)$ and $g_{k'}(t)$ filters to avoid the CP. In non orthogonal MC systems, the transmission of a symbol over the k-th carrier causes the symbol to interfere the adjacent carriers k' at reception through the channel approximated by $\mathbf{H}_{k,k'}$ (see Appendix A).

The particular pattern $\theta_{k',n'}\theta^*_{k,n}$ cause large ICI and ISI interfering terms to belong to the set $\mathcal{I}$ and be completely removed taking the real part, see (6), reducing dramatically interference. At expenses of no perfect orthogonality, FBMC schemes do not require CP, increasing efficiency of the transmission.

3.3 Channel coherency bandwidth

The correctness of the approximation in section above depends on how flat the channel is around the frequencies of interest, measured by coherency. The MIMO channel $\mathbf{h}(t)$ can be coherent or non coherent depending on its power delay profile (PDP). A short effective PDP implies an approximately flat channel, coherent, and then, $\mathbf{H}_{k,k'} \approx \mathbf{H}_{k,k}$, in a small neighborhood of k'.

In the case of perfectly flat channels, $\mathbf{H}_{k,k'} = \mathbf{H}_{k,k}$, all channels share the same singular value decomposition, $\mathbf{u}_{k',l} = \mathbf{u}_{k,l}$, and $\mathbf{v}_{k',l} = \mathbf{v}_{k,l}$. Stream l in k causes no interference in carrier k' whenever $l \neq l'$, due to the orthogonality of beamvectors, $\mathbf{v}^H_{k',l}\mathbf{H}_{k,k}\mathbf{u}_{k,l'} = 0$, $\forall k' \; \forall l' \neq l$. However, when $l' = l$, equivalent channel takes the value $\mathbf{v}^H_{k',l}\mathbf{H}_{k,k}\mathbf{u}_{k,l} = \lambda_{k,l}\sqrt{P_{k,l}}$. Thus, terms with $l' = l$ in set $\mathcal{R}$ and $\mathcal{I}$ contribute to the interference. As, by construction, $\lambda_{k,l} \in \mathbb{R}^+$, there is no change in the real or pure imaginary nature of the interference and all elements in $\mathcal{I}$ can be eliminated with the FBMC scheme, assuming $\hat{H}_{k,l}$ is the actual value of the channel.

However, when $\mathbf{H}_{k,k'} \approx \mathbf{H}_{k,k}$ is only an approximation, beamformer design differs from carrier to carrier. Consequently, streams $l' \neq l$ are not orthogonal any more at carrier k', $\mathbf{v}^H_{k,l}\mathbf{H}_{k,k'}\mathbf{u}_{k',l'} \neq \mathbf{v}^H_{k,l}\mathbf{H}_{k,k}\mathbf{u}_{k,l}$, causing a rise in contribution from set $\mathcal{R}$ and $\mathcal{I}$. Additionally, imaginary terms can leak to the real terms as the quotient $\mathbf{v}^H_{k,l}\mathbf{H}_{k,k'}\mathbf{u}_{k',l'}/\hat{H}_{k,l}$ may be a complex number, modifying the nature of the elements in those sets.

In a non selective channel scenario this quotient has an amplitude close to one and a phase close to 0. Recall that the singular values and vectors of a matrix are continuous functions in small increments of the channel [10], which implies a low leakage in general. When the PDP is longer, the channel is more selective in frequency domain and channels in consecutive carriers cannot be assumed to be similar. Thus, there can be large leakages from $\mathcal{I}$ to $\mathcal{R}$. That will produce ICI and ISI terms that only can be canceled with complex time and frequency post equalizations.

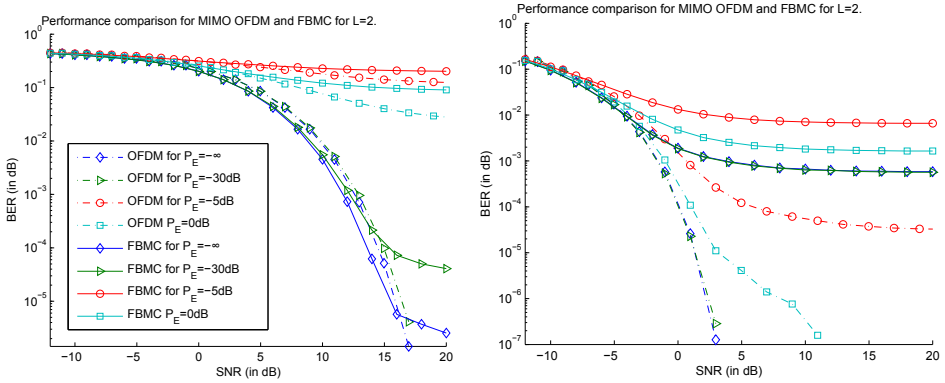

(a) High coherent bandwidth channel. (b) Low coherent bandwidth channel.

Figure 3: Performance comparison for different channel coherence bandwidth and different CSI estimation quality. Both figures share the same legend.

Contrary to FBMC, OFDM does not suffer from those interferences due to the perfect orthogonality between neighbor carriers. So, sets $\mathcal{R}$ and $\mathcal{I}$ are always zero.

3.4 Imperfect channel estimation

In practical systems, the MIMO channel is only available through a channel estimate $\tilde{\mathbf{H}}_{k,k}$ to design the transmit and receive beamformers, $\mathbf{u}_{k,l}$ and $\mathbf{v}_{k,l}^H$. Consequently, there is a mismatch between the actual and the estimated channel, and the actual equivalent channel, $H_{k,l} = \mathbf{v}_{k,l}^H \mathbf{H}_{k,k} \mathbf{u}_{k,l}$, differs from the estimated one, $\hat{H}_{k,l} = \mathbf{v}_{k,l}^H \tilde{\mathbf{H}}_{k,k} \mathbf{u}_{k,l} = \lambda_{k,l}\sqrt{P_{k,l}}$. Effects induced by the estimation mismatch are twofold. On the one hand, in general $\mathbf{v}_{k,l}^H \mathbf{H}_k \mathbf{u}_{k,l'} \neq 0$, as $\mathbf{u}_{k,l'}$ and $\mathbf{v}_{k,l}^H$ are no longer the actual singular values of the channel and cross-interference between streams at the same carrier k appears. However, this is not a critical problem while the estimated channel $\tilde{\mathbf{H}}_k$ is close to the real one $\mathbf{H}_k$.

As $\mathbf{u}_{k,l}$ and $\mathbf{v}_{k,l}^H$ are not the actual singular vectors, $H_{k,l}$ is no longer ensured to belong to real positive numbers. While in general this is not significant for OFDM schemes because $H_{k,l}$ is a small rotation of $\lambda_{k,l}$ in the complex plane, it can become critical for the FBMC scheme as in Section 3.3.

Note that the noise power at stream l in carrier k does not increase although the channel $\tilde{\mathbf{H}}_k$ is used in the design as long as $\mathbf{v}_{k,l}$ are still orthogonal.

4. Simulation

We simulate both OFDM and FBMC schemes in different scenarios to quantify the effects of interferences described. For OFDM the CP has been assumed to be the 20% of the total symbol ($CP = 1/4$). For the FBMC filter design, we select a modular filter scheme truncated at 2048 samples, symbol period $T/T_s = 256$, with T_s the sampling period, and $K = 512$ carriers, proposed by Bellanger in [7] due to its excellent trade-off between time and frequency location with an OQAM modulation based on 2 delayed PAM modulations. A QPSK modulation is used in OFDM and so that rate is the same. We use two streams per carrier, $L = 2$, in a Rayleigh channel MIMO scenario with $n_T = 3$ and $n_R = 3$. The imperfect channel estimation model considered is $\tilde{\mathbf{H}}_k = \mathbf{H}_k + \mathbf{\Delta}_k$, where $\mathbf{\Delta}_k$ is a zero-mean circularly symmetric complex Gaussian random

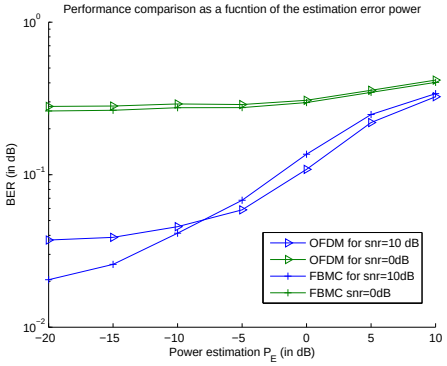

Figure 4: BER Performance in function of estimation error power P_E.

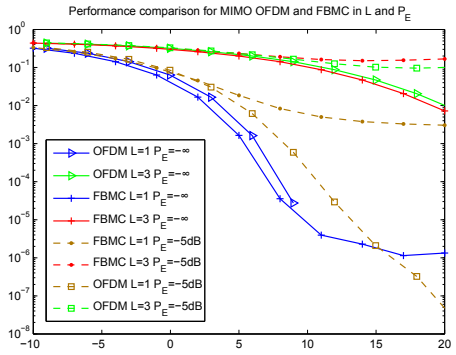

Figure 5: BER performance for different number of streams L with perfect and imperfect CSI.

variable with power equal to P_E. However, results exposed in this paper also holds for other channel modeling. Coherency is modeled by exponential decaying channel with delay spread 2 times the sampling period and another with 50 times.

Figure 3a shows the performance for a high coherent bandwith channel at different P_E values. For perfect CSI, FBMC performs better than OFDM due to the lack of CP. However, FBMC degradates to a minimum error floor even in the perfect CSI case, due to the ICI terms. The same occurs at low P_E power in low SNR. For high P_E values, the degradation in FBMC is faster than OFDM due to higher ICI and ISI terms.

In Figure 3b a longer PDP is considered. The performance of FBMC is only better than OFDM scheme at low SNR levels due to the degradation suffered and the ICI terms from carrier to carrier. Something to highlight is that both BER figures cannot be compared as temporal channel has not been normalized to equivalent gains.

Figure 4 depicts the increase in BER as the power of estimation error increases at different *snr* values. Note that the error is better for OFDM and that there is a crossing in performances for $P_E = -10dB$. That shows that faster degradation in performance of the FBMC scheme. In Figure 5, the BER for FBMC is depicted for different number of streams and CSI qualities. Notice that FBMC performance worsen due to the additional ICI and ISI terms and, unlike OFDM, it saturates even in the perfect CSI case.

5. Conclusions

In this paper we have studied the multistream MIMO-FBMC with modular filters. We have compared the performance of OFDM and FBMC schemes under imperfect CSI and channel frequency coherency. Thanks to the save in the CP, FBMC achieves better performances for a range of SNR. However, there is a degradation even in the perfect CSI case due to the interference between streams. Additionally, this increase is more dramatic for imperfect CSI in comparison to OFDM. Consequently, equalization and robust design techniques are a must to exploit the superior performance of FBMC.

A Effective channel impulse response

We derive the effective MIMO channel of the signals transmitted from filter $f_{k'}(t)$ and received at $g_k(t)$ through the MIMO channel, $g_k(t) * \mathbf{h}(t) * f_{k'}(t)$, where filters $g_k(t)$

are the matched filters of $f_k(t)$. They can be expressed as frequency shifted versions, $g_k(t) = f^*_{k'}(-t)e^{-j2\pi\Delta k\Delta f t}$ where $\Delta k = k' - k$ is separation between carriers. Then,

$$\tilde{\mathbf{h}}_{k,k'}(t) = \int_{-\infty}^{\infty} g_k(\tau) \int_{-\infty}^{\infty} \mathbf{h}(\gamma) f_{k'}(t-\tau-\gamma) d\tau d\gamma = \tag{8}$$

$$= \iiint_{-\infty}^{\infty} f^*_{k'}(-\tau)\mathbf{h}(\gamma)F_{k'}(f)e^{j2\pi f(t-\tau-\gamma)}e^{-j2\pi\Delta k\Delta f\tau} df d\tau d\gamma = \tag{9}$$

$$= \int_{-\infty}^{\infty} F^*_{k'}(f-\Delta k\Delta f)\mathbf{H}(f)F_{k'}(f)e^{j2\pi ft} df \tag{10}$$

where $F_k(f)$ and $\mathbf{H}(f)$ are the Fourier transform of $f_k(t)$ and $\mathbf{h}(t)$, respectively.

When Δk is large, Fourier response of the filters will not overlap in frequency, thus the integral will approximately be zero. However, when Δk is small, assuming that the channel is slowly varying in frequency, the channel matrix can be approximated by its value at the intermediate frequency. After sampling, the remaining integral becomes the transmultiplexer coefficients, $t_{k-k',n}$.

$$\tilde{\mathbf{h}}_{k,k'}(t) \approx \mathbf{H}\left(k\Delta f + \frac{\Delta k}{2}\Delta f\right) \int_{-\infty}^{\infty} F^*_{k'}(f-\Delta k\Delta f)F_{k'}(f)e^{j2\pi ft} df =$$

$$= \mathbf{H}\left(\frac{(k'+k)}{2}\Delta f\right) t_{k'-k,t} = \mathbf{H}_{k,k'}t_{k-k',t} \tag{11}$$

where the last equality is for compactness of notation. Similarly, when $\Delta k = 0$, the channel response is approximated by the value at the filter response, $\mathbf{H}_{k,k}$.

References

[1] G. G.Li, *Orthogonal frequency division multiplexing for wireless communications*. Springer, 2006.

[2] P. Vaidyanathan, "Multirate digital filters, filter banks, polyphase networks, and applications: A tutorial," *Proceedings of the IEEE*, vol. 78, no. 1, pp. 56–93, 1990.

[3] G. Foschini and M. Gans, "On limits of wireless communications in a fading environment when using multiple antennas," *Wireless Personal Communications*, vol. 6, no. 3, pp. 311–335, 1998.

[4] C. Lélé, J. Javaudin, R. Legouable, A. Skrzypczak, and P. Siohan, "Channel estimation methods for preamble-based OFDM/OQAM modulations," *European Transactions on Telecommunications*, vol. 19, no. 7, pp. 741–750, 2008.

[5] M. Payaró, A. Pascual-Iserte, and M. Nájar, "Performance comparison between fbmc and ofdm in mimo systems under channel uncertainty," *Proc. IEEE European Wireless (EW 2010)*, 12-15 April 2010. Lucca (Italy).

[6] D. Palomar, J. Cioffi, and M. Lagunas, "Joint Tx-Rx beamforming design for multicarrier MIMO channels: A unified framework for convex optimization," *IEEE Transactions on Signal Processing*, vol. 51, no. 9, pp. 2381–2401, 2003.

[7] M. Bellanger, "Specification and design of a prototype filter for filter bank based multicarrier transmission," vol. 4, 2001.

[8] P. Siohan, C. Siclet, and N. Lacaille, "Analysis and design of OFDM/OQAM systems based on filterbank theory," *IEEE Transactions on Signal Processing*, vol. 50, no. 5, pp. 1170–1183, 2002.

[9] A. Pascual-Iserte, A. Pérez-Neira, and M. Lagunas, "On power allocation strategies for maximum signal to noise and interference ratio in an OFDM-MIMO system," *IEEE Transactions on Wireless Communications*, vol. 3, no. 3, pp. 808–820, 2004.

[10] J. Magnus and H. Neudecker, *Matrix differential calculus with applications in statistics and econometrics*. Wiley, 1999.

